ISSN 1063-7850, Technical Physics Letters, 2018, Vol. 44, No. 5, pp. 381–383. © Pleiades Publishing, Ltd., 2018.
Original Russian Text © P.A. Alekseev, B.R. Borodin, M.S. Dunaevskii, A.N. Smirnov, V.Yu. Davydov, S.P. Lebedev, A.A. Lebedev, 2018, published in Pis'ma v Zhurnal Tekhnicheskoi Fiziki, 2018, Vol. 44, No. 9, pp. 34–40.

Local Anodic Oxidation of Graphene Layers on SiC

P. A. Alekseev[a]*, B. R. Borodin[a], M. S. Dunaevskii[a], A. N. Smirnov[b], V. Yu. Davydov[a], S. P. Lebedev[a], and A. A. Lebedev[a]

[a] *Ioffe Physical Technical Institute, Russian Academy of Sciences, St. Petersburg, 194021 Russia*
[b] *St. Petersburg National Research University of Information Technologies, Mechanics, and Optics (ITMO University), St. Petersburg, 197101 Russia*
**e-mail: npoxep@gmail.com*

Received January 15, 2018

Abstract—A method of local anodic oxidation has been used to obtain graphene-oxide regions on SiC. The change of the surface properties was confirmed by atomic-force microscopy and Raman spectroscopy. Experimental data were obtained on the conductivity, potential, and topography of the oxidized regions. It was shown that the oxidation leads to a rise in the surface potential. A relationship was found between oxidation parameters, such as the scanning velocity and the probe voltage. The method of local anodic oxidation was used to obtain by lithography an ~20-nm-wide nanoribbon and an ~10-nm-wide nanoconstriction.

DOI: 10.1134/S1063785018050024

Graphene is a layer in which carbon atoms form a 2D hexagonal crystal lattice [1]. Graphene is a promising material for development of new-generation electronic and optoelectronic devices. It is already used to fabricate thin-film transistors [2], OLED displays [3], and many other devices. Large-size wafers of high-quality homogeneous graphene are economically advantageous for numerous applications. The approach the most widely used to obtain large-area graphene is the chemical vapor deposition onto thin metallic foil, with its subsequent transfer to a dielectric substrate. However, the orientation of domains in the thus-grown graphene is random, which impairs its transport characteristics. A high-quality epitaxial graphene with regular orientation of domains can be grown by thermal destruction of a semi-insulating single-crystal SiC substrate [4, 5]. It is a great advantage of this technique that there is no need to transfer a film grown in this way onto a dielectric substrate.

Devices based on graphene are, as a rule, fabricated by photo or electron lithography. In most lithographic procedures, a resist is deposited onto the graphene surface or is removed therefrom. However, the electronic structure of graphene is exceedingly sensitive to structural defects and surface adsorbates, which lowers the carrier mobility [6]. An alternative to lithography, which rules out any use of a resist, is the local anodic oxidation (LAO) [7, 8]. In this method, the surface aqueous film dissociates under the probe of an atomic-force microscope when an electric voltage is applied, with the subsequent oxidation of the graphene layer. The oxidation only occurs where a water meniscus is formed under the probe brought in contact with the surface, and the electronic structure of graphene is not disrupted on the rest of the surface. The possibility of local anodic oxidation of graphene on SiC was demonstrated in [8]. It should be noted that the electronic properties of graphene oxide (GO) on SiC remain nearly unexamined. In addition, low electric voltages and, as a consequence, low probe velocities are used in most studies of this kind with LAO, which hinders lithography on large-area samples. The installation used in the present study makes it possible to apply voltages of up to −50 V. This opens up an opportunity for studies of various oxidation modes at varied voltage and probe velocity. The goal of our study was to examine the graphene oxidation modes and the electronic and structural properties of GO films by atomic-force microscopy (AFM), Kelvin-probe microscopy, and Raman spectroscopy.

Our experiment was performed on an Ntegra Aura (NT-MDT) microscope with DCP (NT-MDT) conducting probes having tip diameter of 100 nm. The sample had the form of a high-quality single-layer graphene with a small fraction (~10%) of two-layer island inclusions of submicron dimensions, produced by thermal destruction of the Si-face of a 6H-SiC (0001) substrate in argon [5]. In measurements of current–voltage (I–V) characteristics and in LAO, the electric voltage was applied between the AFM probe (first electrode) and the pressure contact to the sample surface (second electrode). The humidity level was monitored with a system constructed in the microscope. Raman spectra were measured at room temperature in the backscattering configuration on a Horiba Jobin Yvon T64000 spectrometric installation

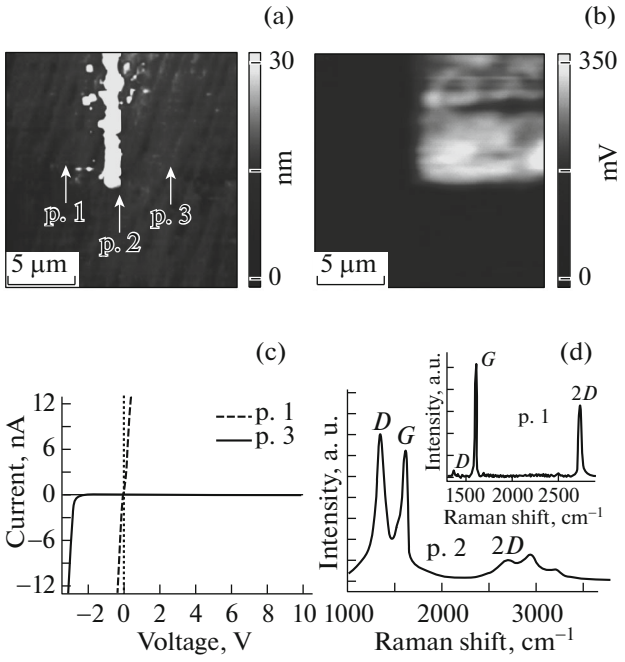

Fig. 1. (a) Topography, (b) surface potential distribution after the treatment, (c) I–V characteristics measured at points p. 1 and p. 3, and (d) Raman spectrum obtained at point p. 2. The inset shows the spectrum obtained at point p. 1.

equipped with a confocal microscope. This made it possible to obtain information from a part of a graphene film with diameter of ~1 μm. The Raman spectra were excited with an Nd:YAG laser (λ = 532 nm).

Figure 1 shows an (a) AFM topographic image and (b) surface-potential-distribution map for part of the surface with an oxidized region in the upper right-hand panel (p. 3). The oxidation was performed at a voltage of –30 V and probe velocity of 1.5 μm/s in the contact mode at a pressing force of 60 nN and relative humidity of 45%. In the oxidation, the fast-scanning axis was horizontal and, therefore, a vertical band was formed at the boundary of the oxidation region in Fig. 1a (p. 2). The appearance of this band was due to the partial transfer of graphene oxide to the boundary of the region in which the oxidation was performed. It can be seen in the surface-potential-distribution map that the region subjected to the treatment has distinct boundaries and its potential is 350 mV higher than the potential unperturbed regions. As is known, the surface potential of SiC without graphene layer is also 350 mV higher than the potential of SiC with a monolayer of graphene. Thus, oxidation of graphene leads to a weaker screening of the SiC potential under graphene.

Figure 1c shows I–V characteristics measured when the probe is brought in contact with the unperturbed and oxidized surface at points p. 1 and p. 3, respectively. The I–V characteristic obtained in the case of a probe in contact with graphene (p. 1) has a linear shape typical of the ohmic contact with a resistance of 30 MΩ. The I–V characteristic measured in the contact of the probe with the oxidized surface (p. 3) exhibits a rectifying (diode) shape typical of a Schottky barrier with n-type semiconductor. It is noteworthy that the oxidized region is insulating relative to the unperturbed surface in a wide range of voltages.

Figure 1d presents a Raman spectrum obtained at the point of accumulation of products formed in the interaction of the probe with the surface (p. 2). The spectrum shows broad bands D (~1345 cm^{-1}), G (~1603 cm^{-1}), and $2D$ (~2692 cm^{-1}) [5]. This spectrum is typical of graphene oxide [9]. Compared with the Raman spectrum of the starting unoxidized graphene layer (it is shown in the inset of Fig. 1d), the GO spectrum is characterized by a significant broadening of the G band and a substantial rise in the intensity of the D band. It is known that the ratio of the integral intensities of the peaks (I_D/I_G) is a measure of the disorder and is inversely proportional to the average size of sp^2 clusters [10, 11]. The increase in this parameter in the GO spectrum points to its higher defectiveness and to a decrease in the size of the sp^2 clusters in GO as compared with the unoxidized layer. In addition, the intensity of $2D$ band in GO is suppressed because of the smaller number of unfaulty atoms with an sp^2 electronic structure. The Raman spectrum of GO shows at high frequencies, in addition to $2D$, several more bands (~2931 and 3188 cm^{-1}) associated with specific features of its electronic structure [9]. Thus, analysis of the Raman spectrum suggests that the graphene surface is modified, which yields graphene oxide.

The humidity strongly affects the oxidation process. The higher the humidity, the lower the probe voltage at which the oxidation occurs. However, a high humidity (~60%) impairs the locality of the process. In this case, the oxidation occurs not only in the region below the probe, but extends to regions with adsorbed water around the probe. The size of these regions may reach several micrometers.

When confirming that graphene oxide is formed in LAO, we examined the oxidation modes (probe voltage and scanning velocity) at a relative humidity of 45%. The most effective mode was that with –15 V and 1 μm/s. This mode combines a moderate probe voltage, a probe velocity sufficient for a fast treatment of large areas, and uniform oxidation of the surface. It is noteworthy that, when the scanning velocity is raised by 1 μm/s, it is necessary to change the probe voltage by –5 V (e.g., 2 μm/s and –20 V, etc.).

The oxidation-mode data enabled us to pass to experiments on obtaining the minimum lithographic resolution. For this purpose, we used probes with a smaller tip radius (NT-MDT: HA_FM/W2C with ~20–30 μm). We performed an experiment on obtain-

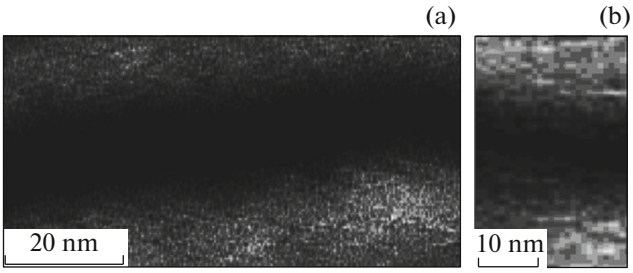

Fig. 2. (a) Graphene nanoribbon (width ~20 nm and (b) graphene nanoconstriction (width ~10 nm) between two oxidized regions.

ing a graphene nanoribbon and a nanoconstriction with as small width as possible. Recently, the authors demonstrated in [12] a record-breaking nanoconstriction with width of 10 nm, obtained on a graphene monolayer produced by mechanical flaking of graphite and transfer to a SiO_2 substrate.

The oxidized region and the gap between these with a linear size of tens of nanometers are, as a rule, detected by measuring the force of probe friction against the surface because the friction between the probe and graphene oxide exceeds that between the probe and graphene [10]. Figure 2 shows friction-force-distribution maps for a part of the surface on which a 20-nm-wide unoxidized graphene nanoribbon (Fig. 2a) and a 10-nm-wide nanoconstriction were formed by the LAO method. This is comparable with the best results obtained on flaked graphite. The light and dark regions in the image correspond to, respectively, oxidized and unoxidized graphene. On performing a set of experiments, we determined the optimal lithographic parameters that provided the best resolution. The lithography was performed in the contact mode at a relative air humidity of ~45%, voltage of –6 V, probe velocity of 0.2 μm/s, and exposure at a point for 10 ms.

Thus, we examined the influence exerted by the parameters (electric voltage and scanning velocity) on the oxidation of graphene monolayers. The parameters providing the reproducible formation of graphene oxide were determined. Experimental data on the conductivity, potential, topography, and crystal structure of the oxidized regions were obtained. The results of the study suggest that the local anodic oxidation of graphene on SiC can be considered a nanolithographic method with a resolution of 10 nm, which can be used to fabricate devices based on thin graphene layers.

Acknowledgments. P.A. Alekseev and B.R. Borodin were supported by a Presidential Grant of the Russian Federation, no. MK-5852.2018.2. S.P. Lebedev was supported by a stipend from the President of the Russian Federation for young scientists and postgraduate students, SP-3472.2016.4.

REFERENCES

1. K. S. Novoselov, A. K. Geim, S. V. Morozov, D. Jiang, Y. Zhang, S. V. Dubonos, I. V. Grigorieva, and A. A. Firsov, Science (Washington, DC, U. S.) **306**, 666 (2004).
2. Y.-M. Lin, K. A. Jenkins, A. Valdes-Garcia, J. P. Small, D. B. Farmer, and P. Avouris, Nano Lett. **9**, 422 (2009).
3. T.-H. Han, Y. Lee, M.-R. Choi, S.-H. Woo, S.-H. Bae, B. H. Hong, J.-H. Ahn, and T.-W. Lee, Nat. Photon. **6**, 105 (2012).
4. K. V. Emtsev, A. Bostwick, K. Horn, J. Jobst, G. L. Kellogg, L. Ley, J. L. McChesney, T. Ohta, S. A. Reshanov, J. Röhrl, E. Rotenberg, A. K. Schmid, D. Waldmann, H. B. Weber, and T. Seyller, Nat. Mater. **8**, 203 (2009).
5. V. Yu. Davydov, D. Yu. Usachov, S. P. Lebedev, A. N. Smirnov, V. S. Levitskii, I. A. Eliseev, P. A. Alekseev, M. S. Dunaevskii, O. Yu. Vilkov, A. G. Rybkin, and A. A. Lebedev, Semiconductors **51**, 1072 (2017).
6. H. S. Song, S. L. Li, H. Miyazaki, S. Sato, K. Hayashi, A. Yamada, N. Yokoyama, and K. Tsukagoshi, Sci. Rep. **2**, 337 (2012).
7. S. Masubuchi, M. Ono, K. Yoshida, K. Hirakawa, and T. Machida, Appl. Phys. Lett. **94**, 082107 (2009).
8. F. Colangelo, V. Piazza, C. Coletti, S. Roddaro, F. Beltram, and P. Pingue, Nanotecnology **28**, 105709 (2017).
9. R. Arul, R. N. Oosterbeek, J. Robertson, G. Xu, J. Jin, and M. C. Simpson, Carbon **99**, 423 (2016).
10. R. Beams, L. G. Cançado, and L. Novotny, J. Phys.: Condens. Matter **27**, 083002 (2015).
11. L. G. Cançado, K. Takai, T. Enoki, M. Endo, Y. A. Kim, H. Mizusaki, A. Jorio, L. N. Coelho, R. Magalhães-Paniago, and M. A. Pimenta, Appl. Phys. Lett. **88**, 163106 (2006).
12. M. Arai, S. Masubuchi, K. Nose, Y. Mitsuda, and T. Machida, Jpn. J. Appl. Phys. **54**, 04DJ06 (2015).

Translated by M. Tagirdzhanov